HHS Public Access

Author manuscript

Equine Vet Educ. Author manuscript; available in PMC 2020 October 09.

Published in final edited form as:

Equine Vet Educ. 2019 October ; 31(10): 517–522. doi:10.1111/eve.12899.

Multifocal discrete osteolysis in a horse with silicate associated osteoporosis

R. Zavodovskaya[1,*], **M. Eckert**[2], **B. G. Murphy**[3], **S. M. Stover**[1], **A. Kol**[3], **S. Diab**[4]

[1]Department of Anatomy, Physiology and Cell Biology, School of Veterinary Medicine, University of California-Davis, Davis, CA 95616 USA

[2]Steinbeck Country Equine Clinic, Salinas, CA 93908 USA

[3]Department Pathology, Microbiology and Immunology, School of Veterinary Medicine, University of California-Davis, Davis, CA 95616 USA

[4]California Animal Health and Food Safety Laboratory, School of Veterinary Medicine, University of California-Davis, Davis CA 95616 USA

Summary

Silicate associated osteoporosis (SAO) was diagnosed *post mortem* in an adult horse with the shortest documented exposure to cytotoxic silicates of 2 years. The horse was evaluated for a 6-months history of progressive back tenderness and acute onset of lameness. The horse had a marked (4/5) [American Association of Equine Practitioners scale] left forelimb lameness, moderate (2/5) hindlimb ataxia and weakness, and cervical pain upon palpation. Physical examination did not reveal clinical skeletal deformities or respiratory compromise. Radiographs revealed widespread, discrete, sharply delineated, osteolytic lesions in the skull, vertebral column, ribs, scapulae and middle phalanx (P2) of the left forelimb and a diffuse bronchointerstitial lung pattern. The presumptive clinical diagnosis was widespread, metastatic osteolytic neoplasia. Due to the poor quality of life and grave prognosis, the horse was humanely euthanised. Post mortem examination revealed pulmonary silicosis in the lungs and hilar lymph nodes and osteolytic lesions with numerous, large osteoclasts and disorganised bone remodeling both consistent with SAO. SAO should be included as a differential diagnosis for horses with widespread, multifocal, discrete osteolysis and history of exposure to endemic regions with possible cytotoxic silicate inhalation. Exposure time of 2 years is potentially sufficient to develop SAO.

[*]**Corresponding author**: rzav@ucdavis.edu.
DR. REGINA ZAVODOVSKAYA (Orcid ID : 0000-0002-8433-3042)

Authors' declaration of interests

The authors declare that there were no conflicts of interest.

Ethical animal research

The horse in this case report was humanely euthanised per the owner's request with consultation from equine veterinarians primarily involved in its care. The horse was not euthanised for the purposes of the larger study into the described disorder.

R. Zavodovskaya contributed to the conception and design of the study, acquisition and interpretation of data and drafting the article. M. Eckert contributed to the conception, acquisition and interpretation of clinical data and critical revision of the article. B. Murphy contributed to conception and design of the study, interpretation of the data and critical revision of the article. S. Stover and A. Kol contributed to the study design, interpretation of the data and critical revision of the article. S. Diab contributed to the conception and design of the study, acquisition and interpretation of data and critical revision of the article. All authors gave final approval of the version of the manuscript to be published.

Keywords

horse; silicosis; osteoporosis; osteoclasts; osteolysis

Introduction

SAO is an enigmatic equine disorder featuring concurrent pulmonary silicosis and osteoporosis (Arens *et al.* 2011). Silicosis is induced by inhalation of cytotoxic, soil-derived crystallised particles of silicate dioxide (e.g. cristobalite) (Arens *et al.* 2011). Granulomas featuring necrosis and fibrosis within the lungs and draining lymph nodes characterise the lesions induced by cristobalite in horses (Schwartz *et al.* 1981; Arens *et al.* 2011). Cristobalite-induced silicosis has also been reported in people and laboratory animals (Mossman and Glenn 2013). Osteoporosis in horses with silicosis is manifested clinically by skeletal deformities (lateral bowing of the scapulae and ribs, lordosis of the spine), skeletal pain (sensitivity to palpation, neck stiffness, and intermittent vague lameness), and pathologic fractures of osteoporotic bones (Anderson *et al.* 2008; Arens *et al.* 2011; Arens *et al.* 2013). SAO-affected horses are geographically clustered in endemic regions where soils are rich in cristobalite (e.g. central California coast) (Arens *et al.* 2011), and cases diagnosed in non-endemic sites had previous exposure to cristobalite-rich soils. The osteoporosis comorbidity has been recognised in horses and implicated in rare reports in humans (Arens *et al.* 2011; Yildizgoren *et al.* 2014; Yildizgoren *et al.* 2016). The pathogenesis of the skeletal manifestation is unknown.

Clinical diagnosis in horses can be challenging and relies on a history of cytotoxic silicate exposure with corresponding clinical findings of skeletal pain and deformities, pathological fractures, and occasional simultaneous respiratory compromise. Ancillary tests used to confirm silicosis and osteoporotic bone changes (i.e. bronchoalveolar lavage, lung biopsy, scapular ultrasound, radiographs, bone scintigraphy) can be informative, although sensitivity and specificity are low (Anderson *et al.* 2008; Arens *et al.* 2013). Gross and histopathologic post mortem examinations remain the gold standard for the diagnosis of SAO. Characteristic lesions in the lung and/or draining lymph nodes include fibrosing granulomas, central necrosis and intralesional refractile crystals. The cristobalite crystals associated with SAO can also be visualised using polarised light microscopy. Fine crystals are more readily observed with transmission electron microscopy (Schwartz *et al.* 1981; Arens *et al.* 2011). Histologic examination of the grossly deformed, osteoporotic bones reveals poorly demarcated areas of osteolysis, disordered remodeling, and mosaic cement lines. The microscopic hallmark of SAO is the presence of numerous, large osteoclasts that create big, scattered cavities in the cortex and medullary trabeculae (Arens *et al.* 2011). Oedema, congestion, haemorrhage and loss of haematopoietic bone marrow are typically observed in areas of active resorption together with increased osteoblastic activity (R. Zavodovskaya, unpublished observations).

Case history

An 8-year-old Paint horse gelding presented with a 6-months history of progressive back tenderness, resistance to saddling, and difficulty walking downhill. A left forelimb lameness had progressed over 3 weeks. The horse had been living in an SAO endemic region for about 2 years. The gelding was moved to a non-endemic location where it resided for approximately 6 months prior to presentation. It was used for pleasure riding.

Clinical findings

At presentation, the horse had a marked (4/5) [AAEP] left forelimb lameness and mild (2/5) [AAEP] hindlimb ataxia and weakness. Cervical pain was noted diffusely, bilaterally throughout the cervical region during palpation of the vertebrae and the articular facet joints. The horse resisted lateral flexion of the neck. Clinical radiographs of the head, cervical, thoracic, and lumbar vertebrae, the distal left thoracic limb and thorax were obtained. Widespread, discrete, sharply delineated, radiolucent lesions, averaging at 1.0 cm and ranging from 0.5 to rare 4.8 cm in diameter were observed throughout the vertebrae, ribs and visible portions of the scapulae (Fig 1). Radiographs revealed a focal, round, 0.7 cm in diameter, subchondral radiolucency at the distopalmar aspect of the middle phalanx (P2) of the left forelimb (Supplementary Item 1). This lesion was not evident on pre-purchase radiographs taken 10 months earlier.

Thoracic radiographs revealed a diffuse bronchointerstitial lung pattern (Fig 2). Mild microcytic normochromic anaemia was the only abnormality identified on the complete blood cell count and serum chemistry profile (HCT 26.6% [30–47%], haemoglobin 10.2 g/dL [10.7–16.5 g/dL], MCV 39.8 fL [41.1–52.4], MCH 15.3 pg [14.1–18.6]). The main presumptive clinical diagnosis was widespread, metastatic osteolytic neoplasia, with SAO being lower on the list of differential diagnoses. Due to the poor quality of life with progressive skeletal pain and grave prognosis, and given the primary differential diagnosis, further tests such as biopsy were not pursued and the horse was humanely euthanised.

Post mortem diagnosis

Post mortem examination revealed hundreds of 1–3 mm diameter, tan, firm granulomas diffusely scattered throughout the pulmonary parenchyma (Fig 2). The hilar (tracheobronchial) and mediastinal lymph nodes, which provide lymphatic drainage from the lung, were markedly enlarged and firm due to central fibrosis and mineralisation. Histologic changes in the lung and lymph nodes were consistent with silicosis characterised by dense, fibrous lesions with central necrosis with occasional dystrophic mineralisation, surrounded by large numbers of histiocytes and multinucleate giant cells, fewer lymphocytes and plasma cells. Sparse, refractile, angular to linear, variably sized (length - 1 to 3μm), intra- and extra-cellular crystals were visualised within granulomas using polarised light (Fig 2).

Gross examination of the skeleton reflected clinical radiographic findings of numerous discrete osteolytic lesions concentrated in the axial portion of the skeleton (skull, vertebral column, ribs) and proximal portions of the appendicular skeleton (scapulae and pelvis) (Fig 1). Rare bone lesions were observed in metaphyseal and epiphyseal regions of long bones

(humerus and P2 of the left forelimb) (Supplementary Item 1). Lesions were discoloured red, circular to rhomboid and sharply demarcated. Similar to radiographic findings, they averaged at 1.0 cm and ranged from 0.5 to 4.5 cm in diameter (Fig 3 and Supplementary Items 1 and 2). On cut surface, red, spongy and friable bone replaced both the cortical and the medullary compartments of the examined bone specimens (Fig 3). Radiographs of dissected specimens demonstrated the sclerotic rim around the lesions (Figs 1 and 3 and Supplementary Items 1 and 2). A rib fracture callus and left stylohyoid bone had poorly defined borders of osteolysis and expansion of the cortical bone with porous bone (Supplementary Item 2). Impression smears of the bone lesions contained mixed bone marrow cell populations along with numerous plump osteoblasts and rare osteoclasts.

Microscopic examination revealed clear demarcation between osteolytic lesions and well-organised parent trabecular and cortical lamellar bone tissue (Fig 3). *De novo,* reparative bone trabeculae characterised by labyrinthine, thin ribbons of intermixed woven and lamellar bone tissue formed in the core of the lesions (Fig 3). The lesional inter-trabecular stroma was predominately hypocellular, oedematous, and congested (Fig 3). Microbial agents or silicate crystals were not identified within skeletal or pulmonary lesions with ancillary tests (Table 1). Serum was tested post mortem with electropherogram due to the radiographic similarity of the skeletal lesions in the examined horse to the lesions in metastatic multiple myeloma, but revealed no abnormality. The diagnosis of SAO was established based on pathological findings in the lungs and bones.

Discussion

This case differs from previously reported SAO cases in 3 important ways. The first distinction is that the previously reported diagnostic skeletal deformities, such as cranial and lateral bowing of the shoulders, were absent (Durham and Armstrong 2006; Anderson *et al.* 2008; Arens *et al.* 2011). Second, the bone lesions, while widespread, were distinctly multifocal and discrete; in contrast to the coalescing to diffuse, poorly demarcated pattern documented previously (Anderson *et al.* 2008; Arens *et al.* 2011; Symons *et al.* 2012). Lastly, this horse developed SAO after the shortest documented exposure to the SAO endemic regions. Previously, the shortest known exposure for SAO development was 4 years, (Arens *et al.* 2011). Records indicated that the horse moved from Nevada (a region where SAO has not been reported) to California and lived 2 years in an SAO endemic region known to have soils rich in cytotoxic silicate. The horse was moved to a non-SAO endemic location 6 months prior to presentation and thus developed the described lesions within 2 years and 6 months.

Widespread, radiographically discrete, radiolucent bone lesions observed in the 8-year-old horse are most consistent with a haematogenously disseminated osteolytic disease, and have not been previously reported in SAO affected horses. Typical osteolytic lesions are poorly demarcated to coalescent accompanied by bone deformity and expansion of the cortex (Arens *et al.* 2011). In this case, the lesions had radiographic features typical of a slowly growing, metastatic neoplasm such as non-productive multiple myeloma (plasma cell myeloma). Other metastatic neoplasms such as melanoma, lymphoma, carcinoma, or Langerhans cell histiocytosis were lower on the list of differential diagnoses. Skeletal pain,

osteolysis, and an axial and proximal appendicular distribution are common to both SAO and metastatic osseous neoplasia (MacAllister *et al.* 1987; Edwards *et al.* 1993; Munoz *et al.* 2009).

Biopsy or needle aspirates of the bone lesions would be useful in differentiating SAO from neoplasia for prognostic and therapeutic purposes. Uniform populations of neoplastic cells, for example plasma cells in potential multiple myeloma or epithelial cells in metastatic carcinoma, would rule out SAO. SAO bone lesion aspirates have not been characterised, but impression smears in the current case contained mixed cell populations with numerous osteoblasts and occasional osteoclasts. Serum hyperglobulinemia with increased immunoglobulin paraproteins on electropherogram would be typical of myeloma (Munoz *et al.* 2009). Electropherogram was normal in the current case. Since some horses affected with SAO respond to bisphosphonate therapy, treatment can be considered in other similar cases where neoplasia and infection have been ruled out (Katzman *et al.* 2012).

An embolic infectious disease was considered unlikely because of the absence of fever, inflammatory leukogram, or lack of reactive bone formation and joint involvement. Infectious pathogens and inflammatory cells were not identified on post mortem impression smears of bone lesions.

The subchondral lesion in the left P2 of the thoracic limb was attributed to SAO based on gross and microscopic findings, and post mortem identification of, grossly similar, subchondral lesions associated with the coxofemoral joints. A focal degenerative joint disease process was ruled out because there were no accompanying degenerative joint disease signs such as joint capsule fibrosis, joint effusion or synovial hyperplasia. Residual abnormality from a developmental disorder was considered unlikely because the lesion was not visualised on radiographs 10 months before presentation. Therefore the lesion in P2 most likely resulted from the same pathological process as the other widespread discrete osteolytic lesions throughout the skeleton.

It is possible that the discrete osteolytic lesions in this case illustrate a previously undocumented early stage or a new manifestation of SAO. With time, the discrete lesions might hypothetically coalesce into the poorly demarcated regions of osteoporosis resembling the later-stage, SAO-typical radiographic and pathologic changes associated with skeletal deformities. In fact, a rib fracture callus and left stylohyoid bone demonstrate the classic SAO lesions (Supplementary Item 2). However, the minimal exposure time and dose of cytotoxic silicates necessary for the initiation and development of the pulmonary and skeletal diseases remain undetermined. Horses suffering from SAO typically present at the terminal stages of osteoporosis because there currently are no sensitive and specific methods to detect the early stages of the slowly progressive and mostly subclinical disease (Arens *et al.* 2013). As a result, end-stage, monophasic bone lesions have historically skewed our understanding of SAO pathobiology to end-stage disease.

The macro and micro-architecture of the polyostotic, but distinct osteolytic lesions were consistent with *embolic* event(s). The polyostotic, circumferential lesion expansion may have progressed from a focus such as a vascular bed. Activation of osteolysis due to a

systemic trigger would likely result in more diffuse lesions. Curiously, the osteolytic lesions target skeletal sites with highly vascular and active hematopoietic bone marrow such as the spine, ribs, scapula and pelvis; similar to skeletal targets of many metastatic cancers (Campbell *et al.* 2015).

The pattern of osteolysis and the skeletal distribution in this case broadens the possibilities of SAO pathogenesis to multifocal, haematogenous “seeding” of a currently undetermined SAO factor or cell with tropism for vascular and bone marrow-rich skeletal sites. The embolic pattern of the osteolytic lesions further challenges a central pathogenic tenet linking the pulmonary and skeletal lesions in SAO. Previously, chronic, excessive osteoclastic activation was theorised to be due to circulating pro-inflammatory factors generated in the extra-skeletal silicotic granulomas (Arens *et al.* 2011). Extra-skeletal inflammatory disease-derived factors like cytokines TNFα (tumour necrosis factor alpha) and/or IL1 (Interleukin-1) have been implicated in osteoporosis comorbidity through potentiation of osteoclastogenesis and osteoclast activation in a number of conditions, including chronic obstructive pulmonary disease (COPD) (Takayanagi 2007; Chen *et al.* 2015). However, the osteolysis in this case is not generalised, but multifocal and more consistent with an initial embolic distribution of the osteolytic trigger. The skeletal distribution of the bone lesions in this case indicates targeted rather then random distribution of the osteolytic trigger throughout the skeletal vascular beds. Therefore, a previous theory of skeletal dissemination of silicate-laden macrophages migrating from the thorax as initiators of osteolysis may need to be re-examined (Arens *et al.* 2011).

In summary, SAO should be considered as a differential diagnosis in horses with widespread, multifocal, discrete osteolytic lesions lacking fever, hypercalcemia and serum protein alterations. Evaluation of environmental factors, such as location of farm for possible exposure to cytotoxic silicate particles, should be pursued in the initial steps of exploration of this diagnosis. Biopsy or cytological aspirates of the osteolytic lesions may be helpful to rule out metastatic neoplasia. This is the first report of a case with discrete osteolysis in SAO where multifocal bone lesions are most consistent with an embolic rather than systemic osteolytic process. The underlying biologic variations in this horse such as genetic background, immunological status and environmental factors may influence the unique presentation of this SAO case and cannot be ruled out. There is a need for *ante mortem* diagnostic tests to identify early stages of disease, which would facilitate the epidemiological studies of risk factors. The underlying cause(s) for the dysregulated bone lysis and inadequate repair in equine SAO remains unknown.

Supplementary Material

Refer to Web version on PubMed Central for supplementary material.

Acknowledgments

We thank Dr Durham (Steinbeck Country Equine Clinic, Salinas, California, USA), for providing his clinical expertise on the case. Consultations and review of the case with Dr. Roy Pool (College of Veterinary Medicine, Texas A&M University, College Station, Texas USA), fueled the development of ideas in this manuscript.

Sources of funding

This project was supported by the Center for Equine Health with funds provided by the State of California pari-mutuel fund and contributions by private donors, and T32 NIH comparative medicine training grant.

Abbreviations

SAO	Silicate Associated Osteoporosis
AAEP	American Association of Equine Practitioners scale
P2	Middle phalanx

References

1. Anderson JD, Galuppo LD, Barr BC, Puchalski SM, Macdonald MM, Whitcomb MB, Magdesian KG, Stover SM. 2008; Clinical and scintigraphic findings in horses with a bone fragility disorder: 16 cases (1980–2006). J. Am. Vet. Med. Assoc. 232:1694–1699. [PubMed: 18518812]
2. Arens AM, Barr B, Puchalski SM, Poppenga R, Kulin RM, Anderson J, Stover SM. 2011; Osteoporosis associated with pulmonary silicosis in an equine bone fragility syndrome. Vet. Pathol. 48:593–615. [PubMed: 21097716]
3. Arens AM, Puchalski SM, Whitcomb MB, Bell R, Gardner IA, Stover SM. 2013; Comparison of the use of scapular ultrasonography, physical examination, and measurement of serum biomarkers of bone turnover versus scintigraphy for detection of bone fragility syndrome in horses. J. Am. Vet. Med. Assoc. 242:76–85. [PubMed: 23234285]
4. Campbell BA, Callahan J, Bressel M, Simoens N, Everitt S, Hofman MS, Hicks RJ, Burbury K, MacManus M. 2015; Distribution Atlas of Proliferating Bone Marrow in Non-Small Cell Lung Cancer Patients Measured by FLT-PET/CT Imaging, With Potential Applicability in Radiation Therapy Planning. Int. J. Radiat. Oncol. Biol. Phys. 92:1035–1043. [PubMed: 26194679]
5. Chen SJ, Liao WC, Huang KH, Lin CL, Tsai WC, Kung PT, Chang KH, Kao CH. 2015; Chronic obstructive pulmonary disease is a strong independent risk factor for osteoporosis and pathologic fractures: a population-based cohort study. QJM. 108:633–640. [PubMed: 25614611]
6. Durham, M; Armstrong, CM. Fractures and bone deformities in 18 horses with silicosis; Proceedings. 52nd Annual Convention of the American Association of Equine Practitioners; 2006. 311–317.
7. Edwards DF, Parker JW, Wilkinson JE, Helman RG. 1993; Plasma cell myeloma in the horse. A case report and literature review. J. Vet. Intern. Med. 7:169–176. [PubMed: 8331611]
8. Katzman SA, Nieto JE, Arens AM, MacDonald MH, Puchalski SM, Galuppo LD, Snyder JR, Maher O, Bell RJ. 2012; Use of zoledronate for treatment of a bone fragility disorder in horses. J. Am. Vet. Med. Assoc. 240:1323–1328. [PubMed: 22607600]
9. MacAllister C, Qualls C Jr, Tyler R, Root CR. 1987; Multiple myeloma in a horse. J. Am. Vet. Med. Assoc. 191:337–339. [PubMed: 3654300]
10. Mossman BT, Glenn RE. 2013; Bioreactivity of the crystalline silica polymorphs, quartz and cristobalite, and implications for occupational exposure limits (OELs). Crit. Rev. Toxicol. 43:632–660. [PubMed: 23863112]
11. Munoz A, Riber C, Trigo P, Castejón F. 2009; Hematopoietic neoplasias in horses: myeloproliferative and lymphoproliferative disorders. J. Equine Sci. 20:59–72. [PubMed: 24833969]
12. Schwartz LW, Knight HD, Whittig LD, Malloy RL, Abraham JL, Tyler NK. 1981; Silicate pneumoconiosis and pulmonary fibrosis in horses from the Monterey-Carmel peninsula. Chest. 80:82–85. [PubMed: 7249751]
13. Symons JE, Entwistle RC, Arens AM, Garcia TC, Christiansen BA, Fyhrie DP, Stover SM. 2012; Mechanical and morphological properties of trabecular bone samples obtained from third metacarpal bones of cadavers of horses with a bone fragility syndrome and horses unaffected by that syndrome. Am. J. Vet. Res. 73:1742–1751. [PubMed: 23106459]

14. Takayanagi H. 2007; Osteoimmunology: shared mechanisms and crosstalk between the immune and bone systems. Nat. Rev. Immunol. 7:292–304. [PubMed: 17380158]
15. Yildizgoren MT, Ekiz T, Nadir Ozis T, Baki AE, Tutkun E, Ozgirgin N. 2014; Osteoporosis: can it be related to silicosis? Tuberk. Toraks. 62:98–99. [PubMed: 24814085]
16. Yildizgoren MT, Ozis TN, Baki AE, Tutkun E, Yilmaz H, Tiftik T, Ekiz T, Ozgirgin N. 2016; Evaluation of bone mineral density and 25-hydroxyvitamin D levels in subjects with silica exposure. Environ. Health Prev. Med. 21:149–153. [PubMed: 26825971]

Fig 1.

A – Lateral radiographs demonstrated discrete, circular to ovoid osteolytic lesions (white arrow) in the angle of the mandible, B – second and third cervical vertebrae and C – thoracic spinous processes. C – Faint outlines of osteolytic lesions were visible in the overlying dorsal aspect of the scapula (outline of the dorsal border and spine of the scapular are marked with black arrows). An outer radiodense rim accentuated the osteolytic lesions throughout the skeleton.

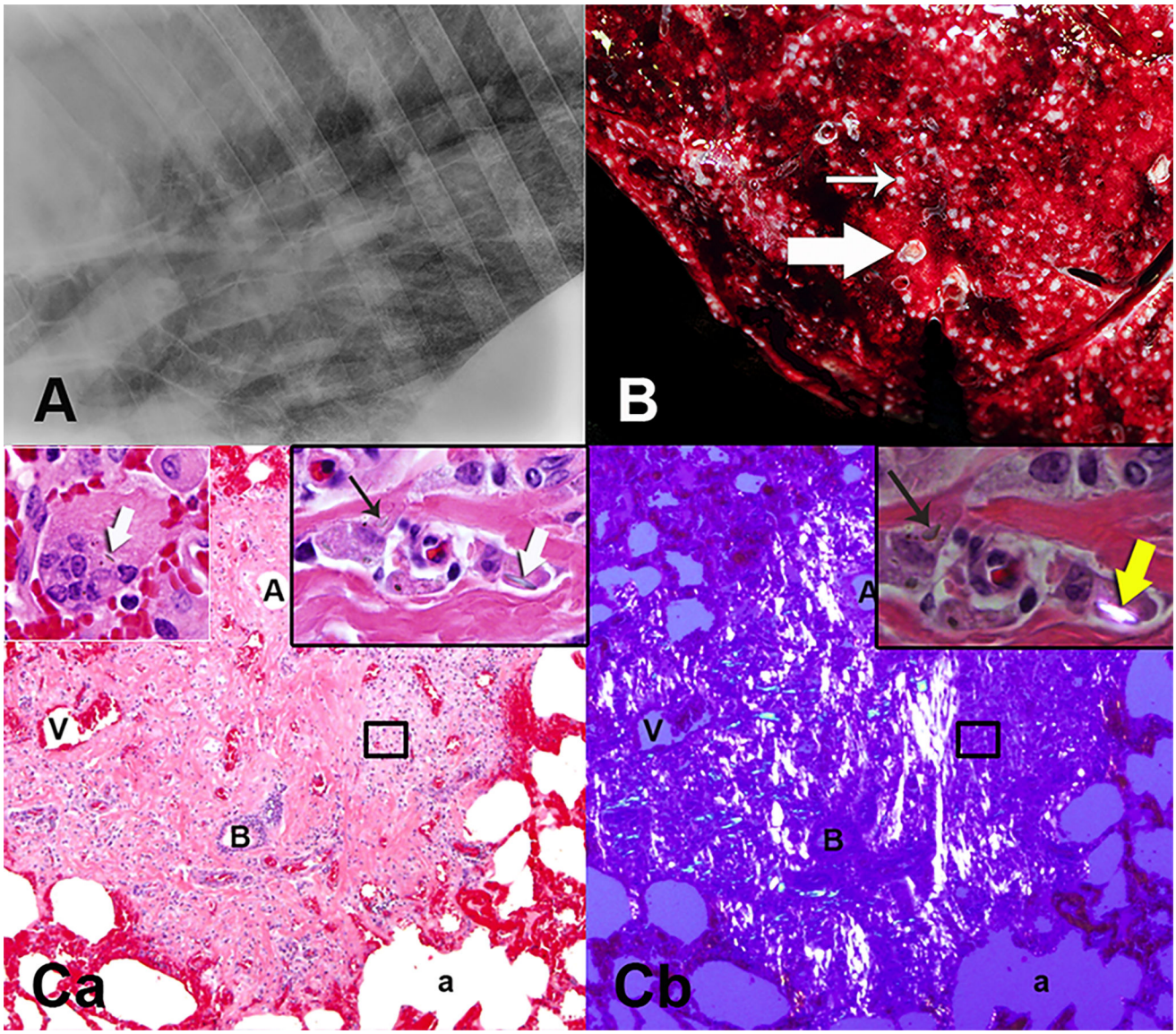

Fig 2.

A – Lateral radiograph of the caudal lung field demonstrated diffuse interstitial lung pattern. B – Miliary granulomas (thin arrow) were scattered throughout the lung parenchyma as shown on the cut surface of the gross specimen (histology Ca,b). Some of the small bronchi were plugged with mucus and inflammatory cells (thick arrow). Ca - The granulomas were next to or surrounded terminal bronchi (B) characterised by numerous macrophages within abundant fibrosis. Cb - Polarising filters highlighted the bright, streaming, autofluorescent fibrous bands within the granuloma. Ca,b inserts - Many macrophages contained sharp fragments of crystalline particles (thick arrows), some of which were highlighted with polarisation (yellow arrow). Ca - Upper left insert shows crystalline particle in a multinucleated macrophage. Alveolar (a) walls and vessels were red due to congestion. (A – arteriole, V – vein) (H&E)

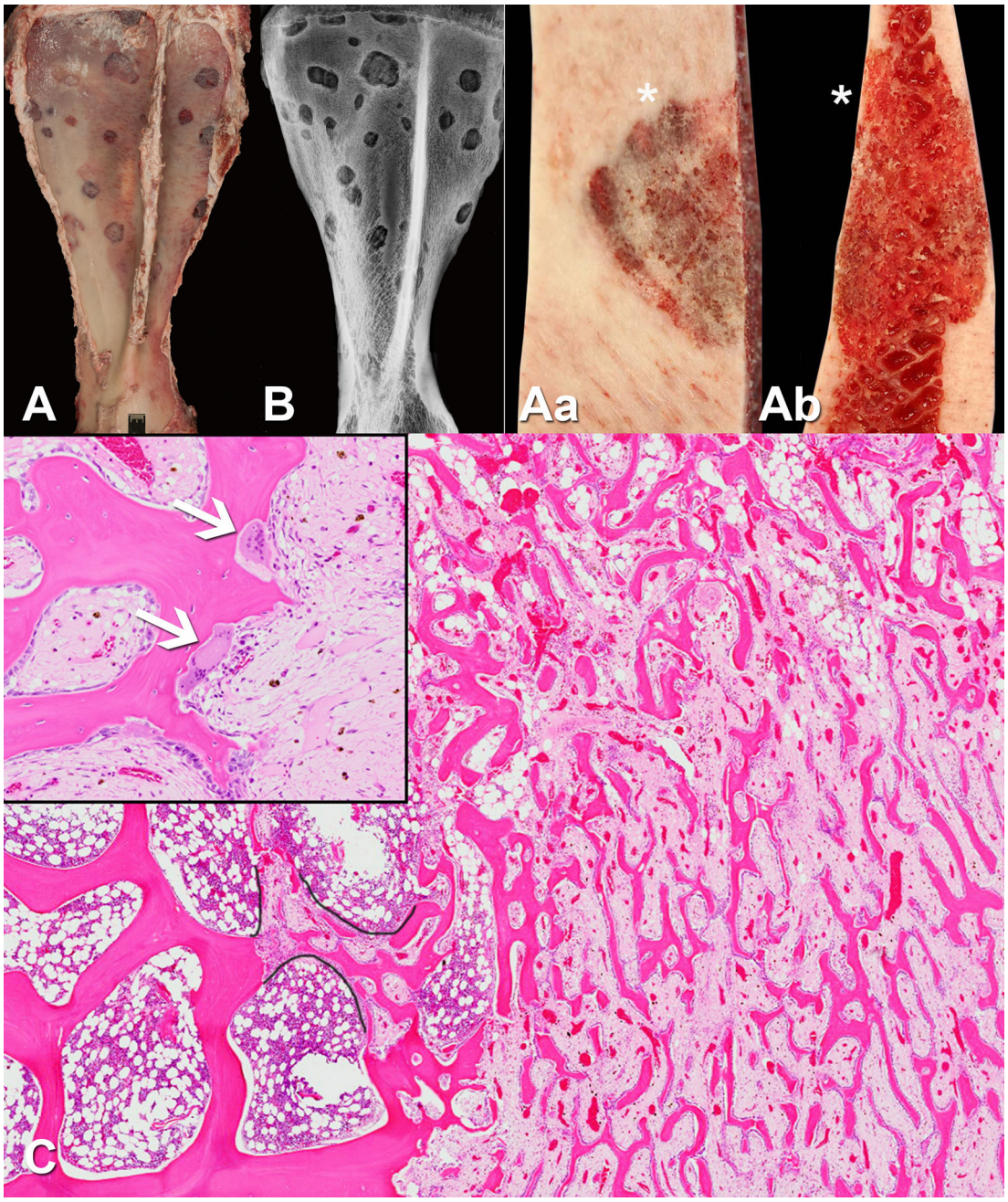

Fig 3.

The panel illustrates gross and histological features of the discrete, osteolytic lesions found predominately in the axial and proximal appendicular skeletal sites. A - Left scapula, abaxial surface, and B – lateromedial postmortem radiograph, illustrate the numerous rounded to rhomboid, well-demarcated osteolytic lesions. B – A peri-lesional sclerotic rim is consistent with a short transition zone. Aa – Closer view of the surface and Ab - transverse section of one of the scapular lesions demonstrated replacement of smooth cortical surface and medullary trabecular network by friable, porous, almost spongy, bone tissue. The asterisks indicate abaxial surface of the scapula. C – Micrograph of a representative bone lesion

demonstrated thick, organized trabeculae (left half of image) adjacent to a thin, labyrinthine network of intralesional trabeculae (right half of image) that make up the spongy bone. The spongy bone replaced medullary and cortical bone. Characteristic of SAO, morphologically atypical, large and numerous osteoclasts (arrows) were frequently observed at the bone surfaces (insert demonstrates the hyperactive osteoclasts seen in SAO). The stroma between the spongy bone trabeculae was marked by oedema, congestion, haemorrhage and loss of haematopoietic bone marrow. Black outlines highlighted ongoing repair of resorbed segment of trabecular bone. Note the respected boundaries between thin anastomosing trabeculae within fibrous stroma and surrounding bone marrow elements in this repair. (H&E)

Table 1

Ancillary tests performed during investigation of this case are summarized.

Test	Tissue	Result
KOH (potassium hydroxide) wet mount	Lung impression smears	Negative for fungal spherules suggestive of *Coccidioides* sp
Cytology (Diff-Quik)	Rib osteolytic lesions impression smears	Negative for infectious agents, neoplastic or inflammatory cells
Fungal and aerobic bacterial cultures	Lung and hilar lymph nodes tissues	Negative growth
Hematoxylin and eosin, Gram, Periodic acid–Schiff (PAS), and acid fast stains	Lung and hilar lymph nodes histological sections	Negative for infectious organisms
Serum electrophoresis	Frozen serum	Normal
Transmission electron microscopy (TEM)	Osteolytic lesion – rib, vertebra, and stylohyoid bones	Putative etiological agent(s) not observed